June 2009 *Volume 5 Issue 3*

Trade Science Inc.

Materials Science

An Indian Journal

Full Paper

MSAIJ, 5(3), 2009 [168-174]

Sol-gel synthesis of TiO_2 nanoparticles with different surfactants and their photocatalytic activity

Ammar Elsanousi*, H.M.H.Fadlalla, Jun Zhang, Feng-Jun Shi, Xiaoxia Ding, Zhixin Huang, Chengcun Tang*

College of Physical Science and Technology, Central China Normal University, Wuhan, 430079, (P.R.CHINA)

Fax : 86-27-67861185

E-mail : a.elsanousi@phy.ccnu.edu.cn

Received: 11th May, 2009 ; Accepted: 16th May, 2009

ABSTRACT

Titania nanoparticles were synthesized by sol-gel technique with and without the addition of surfactant. Two types of surfactants were used as particle size inhibitors: Cetyltrimethylammonium bromide (CTAB) and polyvinylpyrolidone (PVP). The samples were characterized and their photocatalytic activity was measured and compared to Degussa P-25 nanopowder. Results showed that the prepared nanoparticles show different particle size, particle size distribution and phase composition. Samples prepared by using CTAB as surfactant reveal pure anatase phase structure with uniform size distribution of about 13 nm, while samples prepared without the introduction of surfactant and those prepared by using PVP expose a bi-phase structure with different rutile concentration and particle size distribution. The highest degradation efficiency was obtained by the photocatalyst prepared with PVP as surfactant; while the lowest degradation efficiency was obtained by the photocatalyst prepared using CTAB. The bi-phase powders show higher degradation efficiency compared to pure anatase phase powders, probably due to a synergetic effect between anatase and rutile powders, which enhances the electron-hole separation and thus increases the photocatalytic activity.

KEYWORDS

TiO_2;
Bi-phase;
Photocatalytic activity;
Surfactant;
Synergetic effect.

1. INTRODUCTION

Semiconducting nanocrystalline materials are of great interest due to their unique properties. Among these materials, ultrafine nanostructured materials with crystallite sizes smaller than 100 nm and high surface areas have attracted much attention due to their unusual optical, electrical, and catalytic properties. It was reported that decreasing the particle size of the nanomaterial leads to an enhancement in the catalytic activity because the optical band gap is widened due to the quantum size effect, combined with the increased surface area[1-6].

Recently, strong efforts have been made to develop metal oxide semiconductor materials with active optical properties, for enhanced optoelectronic, and photocatalytic applications. As an n-type semiconductor with a wide energy band gap, titanium dioxide (TiO_2) has been extensively used in a variety of applications such as solar energy conversion, photocatalysis and gas

sensing because of its high photocatalytic activity, excellent optical transmittance, high refractive index and chemical stability[7-10]. TiO_2 has three main crystal phases: anatase; rutile and brokite[11,12]. Among these phases, anatase phase, which is a meta-stable phase, is also chemically and optically active proved to be suitable for photocatalyst. Anatase TiO_2 is also known for its ability to act as an electrode material for light-sensitizers in dye-sensitized solar cells, where it was found that photo-electrodes prepared using anatase phase TiO_2 results in better photoconversion efficiency compared to other crystal structures due to its high photoactivity [13,14]. Rutile phase is known as white pigment because of its high scattering effect which leads to protection from the ultraviolet light.

The photocatalytic activity is considered as an important characteristic of TiO_2. According to the principles of semiconductor TiO_2 photocatalysis, the photocatalytic activity is mainly dependent on the electron–hole generation capacity, electron transfer route and separation efficiency of photo-generated charge pairs[15]. Generally, the optical and electrical properties of TiO_2 nanoparticles depend strongly on the morphology, particle size, particle size distribution, phase composition, surface area and porosity of the resultant material. Therefore the precise control of these factors is of basic importance for determining the properties of the final material. In recent years, a wide variety of techniques have been developed to produce TiO_2 nanoparticles like hydrothermal method in which amorphous TiO_2 , $TiCl_4$ or $TiOCl_2$ aqueous solution are used[16,17]. TiO_2 nanoparticles can also be produced by hydrolysis of titanium compounds, such as titanium tetraisopropoxide (TTIP), titanium tetrachloride ($TiCl_4$) or titanium alkoxides (Ti(OR)4)[18,19]. However, using chlorine containing starting materials or organic ligand usually results in the residue containing chlorine or carbon in the as-prepared powder which limits the use of the product for different applications and can also have some environmental impact. The sol–gel technique has been regarded as an excellent method for the synthesis of nanosized metal oxides and has been widely employed for the preparation of TiO_2 nanoparticles. One of the advantages of sol-gel technique is that the particles size, shape and crystalline phase can be controlled by the addition of surfactants during the preparation processes[20,21].

The ultimate goal of this study is to enhance the photoactivity of TiO_2 nanoparticles through the manipulation of particle shape, size and crystal structure by using different surfactant types. In this study, different TiO_2 nanoparticles were prepared through the sol-gel technique at room temperature with and without the introduction of surfactants and a comparison between the morphological structure and photocatalytic activity of the synthesized nanoparticles was performed.

2. EXPERIMENTAL

2.1. Materials

Tetrabutyl titanate ($C_{16}H_{36}O_4Ti$) was used as the precursor compound for the sol-gel process. Cetyltrimethylammonium bromide (CTAB) and polyvinylpyrolidone (PVP) were used as surfactants. All chemicals and solvents were purchased from Shanghai Chemical Reagent Company (China) and were used without further purification.

2.2. Preparation of TiO_2 nanoparticles

Three samples of TiO_2 nanoparticles were prepared by the sol-gel technique. The first sample (which will be denoted hereafter as CTAB-TiO_2) was prepared by using CTAB as surfactant. The typical process is as follows: 23 ml of tetrabutile titanate was added to 23ml of ethanol and the resulting solution (sol. 1) was stirred for 30 minutes. 0.3g of CTAB was dissolved in 23 ml of ethanol, then added to 18g of 4.4M HCl aqueous solution and stirred for 15 minutes (sol. 2). Sol. 2 was added dropwise to the former solution (sol. 1) under vigorous stirring at room temperature. The resulting mixture was held for hydrolysis in an incubator at 40 oC for 4 days. The obtained gel was then milled and annealed at 600^0C for 2 hours with heating and cooling rates of $\pm 20^0$C. The second sample (PVP-TiO_2) was prepared following the same route, but by using PVP instead of CTAB as surfactant. For the comparison purposes, a third sample (N-TiO_2) was prepared without using any surfactant.

2.3. Characterization

The crystal phase composition of the samples were characterized by powder X-ray diffraction (XRD; D/

Full Paper

max-RB) using a Bruker D8 diffractometer with Cu kα radiation (λ =0.154178 nm). XRD patterns were obtained for the 2θ range 20-80° by step-scanning with a step size of 0.06^0C. To determine the average crystallite size, peak broadening analysis was applied to anatase and rutile diffraction peaks using Scherrer's equation. The morphology and grain size of the titania particles were examined by scanning electron microscopy (SEM, JEOL JSM-6700F). The powder samples were ultrasonically dispersed in ethanol and transferred onto carbon-coated copper grids for the transmission electron microscopy (TEM, JEOL, JEM-2010F).

2.4. Photocatalytic activity measurements

The photocatalytic activities of the synthesized TiO_2 powders were evaluated by measuring the decomposition rate of methyl orange (MO) at room temperature, and compared with the activity of the commercial TiO_2 powder (P-25, Degussa). 0.08g of the sample powder was ultrasonically dispersed in 80 ml of aqueous MO solution with the concentration of 20mg/L at the natural pH value. The mixture was placed in an ultrasonic bath for 10 minutes to form a suspension and then was placed in the dark under continuous magnetic stirring. A UV-lamp (λ = 360 nm) was fixed about 20cm above the surface of the solution as light source and small quantities of the solution were withdrawn after various reaction times (0, 5, 15, 25, 40 and 60 minutes). Each sample solution was centrifuged at 4000 rpm for 10 minutes in order to separate the catalyst particles from the solution. The absorption spectra were recorded between 200 and 800 nm using a UV-vis spectrophotometer and the residual concentration of MO was determined by measuring the maximum absorption peak value of each sample solution at approximately 464 nm.

3. RESULTS AND DISCUSSION

3.1. Characterization results

Figure 1 shows the X-ray diffraction patterns of TiO_2 nanoparticles prepared with different surfactants. The diffraction peaks in all samples obviously correspond to crystalline titanium dioxide of either anatase or rutile phase.

The XRD pattern of the nanoparticles prepared by using CTAB as surfactant (CTAB-TiO_2) expose a similar

TABLE 1: Average particle sizes of samples calculated by Scherrer's equation

Sample	Average particle size (nm)	Crystal structure	
		Phase	Rutile (%)
CTAB-TiO_2	13	anatase	0
PVP-TiO_2	17	anatase/rutile	28
N-TiO_2	28	anatase/rutile	90
P-25	21	anatase	0

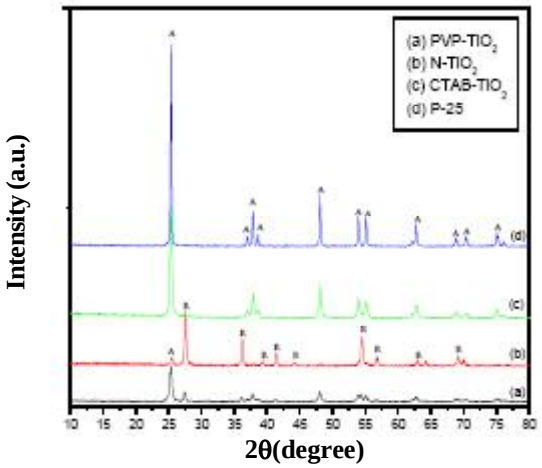

Figure 1 : X-ray diffraction patterns of TiO_2 nanoparticles prepared with different surfactants compared with Degussa P-25 nanopowder

crystalline structure to the commercial TiO_2 nanopowder (P-25) with pure anatase phase (figure 1(c) and (d)), while the patterns of the samples prepared without the addition of surfactant (N-TiO_2) and those prepared by using PVP as surfactant (PVP-TiO_2), both show crystalline structures with mixed phase of anatase and rutile crystals (see figure 1 (a) and (b)). The phase composition of these samples was calculated from the equation[22]:

$$X_R = 1 - \left[1 + 1.26\left(\frac{I_R}{I_A}\right)\right]^{-1} \quad (1)$$

where X_R is the weight fraction of rutile in the mixture, and I_R and I_A are the peak intensities of the rutile (110) and anatase (101) diffractions, respectively and the results are listed in TABLE 1.

The average particle size of crystalline TiO_2 was roughly estimated by calculation from the width of the XRD peaks using the Scherrer equation:

$$D = \frac{k\lambda}{\beta\cos\theta} \quad (2)$$

where k is a constant (0.94), λ is the XRD wavelength, β is the

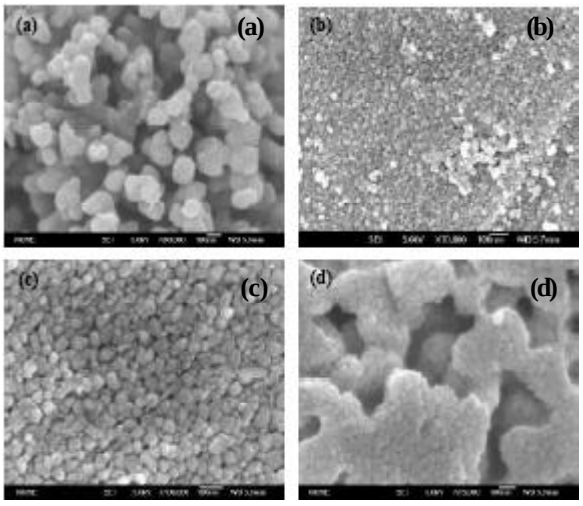

Figure 2 : SEM images of TiO_2 nanoparticles prepared with and without different surfactants: (a) CTAB-TiO_2, (b) PVP-TiO_2, (c) and (d) N-TiO_2

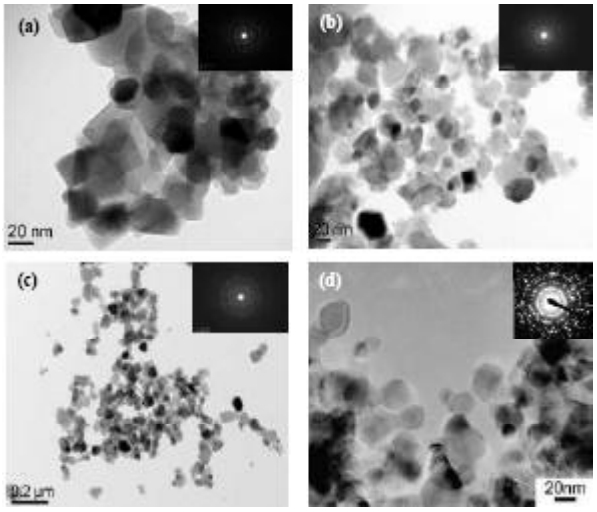

Figure 3 : TEM micrographs of TiO_2 nanoparticles prepared with and without different surfactants: (a) CTAB-TiO_2, (b) PVP-TiO_2, (c) N-TiO_2 and (d) P-25[24]

corrected half-width of the strongest diffraction peak and θ is the diffraction angle. The average particles size of the powders; CTAB-TiO_2, PVP-TiO_2, N-TiO_2 and P-25 are summarized in TABLE 1.

From this TABLE, it is apparent that the presence of both surfactants resulted in decreasing the size of the formed nanoparticles, although CTAB shows a better ability in decreasing the nanoparticles size compared to PVP. This can be ascribed to the fact that the surfactant molecules form an organic shell on each single particle preventing the coalescence of the nanocrystals and the growth of bigger particles by reducing the surface tension, i.e. it provides a cage-like effect that limits particle nucleation, growth and agglomeration. In this sense, the CTAB which has a shorter chain length seems to be more effective than PVP, probably due to a better coating of the particles[23].

Figure 2 shows the SEM images of TiO_2 nanoparticles prepared with and without the addition of surfactants. Large aggregates of fine particles with an average particle size of about 13 nm and a uniform particle size distribution was observed in sample CTAB-TiO_2 (Figure 2(a)). Sample PVP-TiO_2 shows a mesoporous structure with pore diameter of about 10nm and a relatively large particle size distribution in the range between 15-35 nm as can be seen from figure 2(b). The sample prepared without the presence of any surfactant (N-TiO_2) shows a similar aggregated structure to CTAB-TiO_2, however, the sample also shows a very large particle size distribution in the range between 20-50nm (see figure 2(c) and (d)). This broadened particle size distribution in PVP-TiO_2 and N-TiO_2 samples can be attributed to the biphase structure of anatase and rutile crystals existing in both samples.

In order to confirm the morphological structure and identity of the resulting products, TEM analysis was performed for all samples. The TEM micrographs of the three samples (CTAB-TiO_2, PVP-TiO_2 and N-TiO_2) are shown in figures 3 (a-c) respectively. Figure 3(d) presents the TEM micrograph of the commercial P-25 (Degussa) nanopowder. The nanoparticle size and particle size distribution show a good agreement with the SEM analysis.

The selected area electron diffraction (SAED) analysis shows a polycrystalline structure for all samples, as indicated by the ring pattern in the inset of each image in figure 3. The lattice spacing (d) was calculated for all produced nanopowders and was found to be 0.350 nm and 0.356 nm for the CTAB-TiO_2 and PVP-TiO_2 samples respectively, which corresponds to the anatase phase (101) according to the pdf card number[21-1272]. The calculated lattice plane spacing for the N-TiO_2 was found to have a value of about 0.325 nm corresponding to the rutile phase (110) according to the pfd card number[21-1276].

These results match well with the phase composition calculations made by equation 1. Although the phase composition calculated from equation 1 shows a biphase structure for N-TiO_2 and PVP-TiO_2 samples,

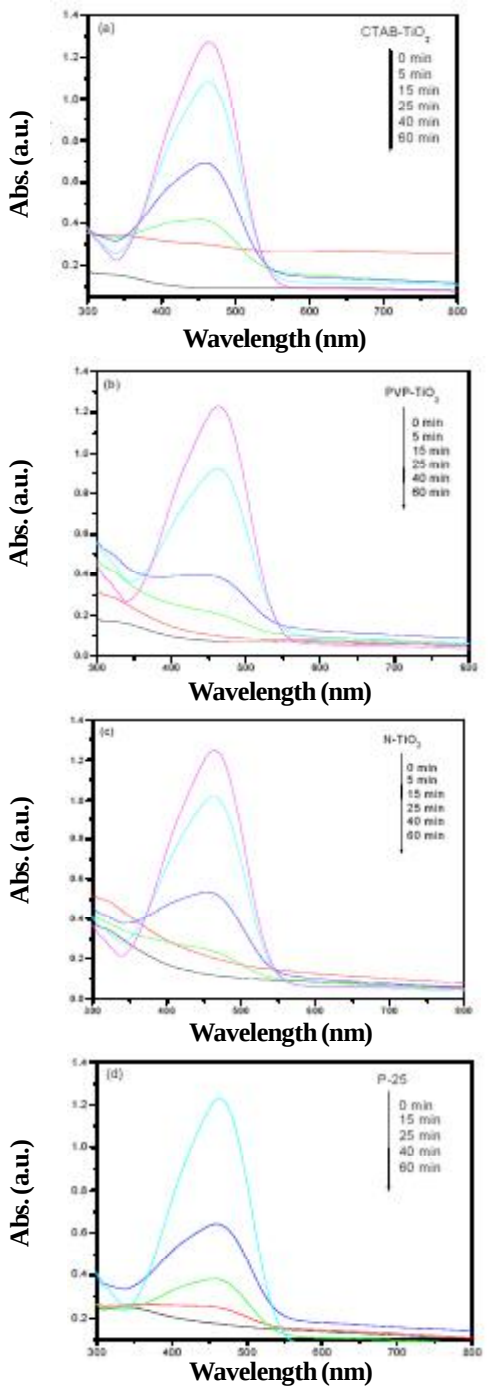

Figure 4 : UV–vis absorption spectra of MO/photocatalyst samples with different reaction time under UV irradiation for the samples: (a) CTAB-TiO_2, (b) PVP-TiO_2, (c) N-TiO_2 and (d) P-25

but the calculation of the phase composition from the SAED pattern can only show the composition of the dominant phase, which is 90% rutile phase for N-TiO_2 sample and 72% anatase phase for the PVP-TiO_2 sample (see TABLE 1).

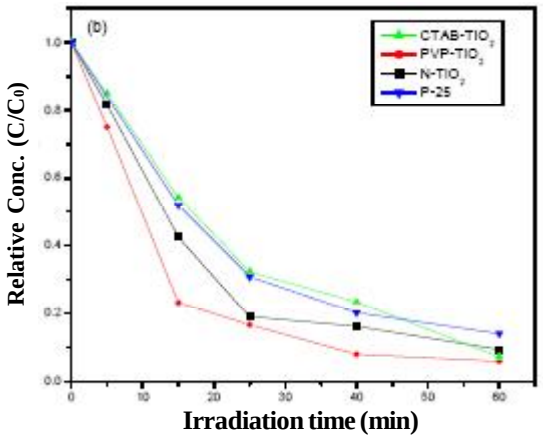

Figure 5 : Photocatalytic degradation of MO on various TiO_2 photocatalysts (original MO concentration: 20 mg/L; photocatalyst concentration: 1 g/L)

3.2. Photocatalytic degradation of MO

The photocatalytic activity of the synthesized nano powders was studied by investigating the degradation of methyl orange (MO) in the presence of the CTAB-TiO_2, PVP-TiO_2, N-TiO_2 and P-25 photocatalysts at various time intervals. Figure 4 shows the UV–vis absorption spectra of MO on different photocatalysts with different reaction time under UV irradiation. From this figure it was observed that the concentration of MO in all reaction systems decreases with the photocatalysis processing time.

Figure 5 shows the Photocatalytic degradation of methyl orange on different photocatalysts. Observations show that the photocatalytic activity varies with the type of the photocatalyst. The highest degradation efficiency was reached with the photocatalyst PVP-TiO_2, while the photocatalyst CTAB-TiO_2 shows the lowest degradation efficiency, although it contains the smallest particle size.

The photocatalytic degradation of methyl orange is supposed to follow the pseudo first-order reaction kinetics which can be expressed as follows:

$$\ln\left(\frac{C_0}{C}\right) = kt \qquad (3)$$

where k is the reaction rate constant, C_0 and C are the initial concentration and the reaction concentration of methyl orange, respectively.

The reaction rate constant was calculated for the different photocatalysts using equation 3 and the values are listed in TABLE 2.

TABLE 2 : Reaction rate constants for the different photocatalysts

Sample	Reaction rate constant k (min^{-1})
PVP-TiO_2	0.05938
N-TiO_2	0.04597
P-25	0.03922
CTAB-TiO_2	0.03725

According to the pseudo first-order kinetics, it was observed that the photocatalysts with the bi-phase structure (PVP-TiO_2 and N-TiO_2) show higher reaction rates compared to the pure anatase phase photocatalysts (CTAB-TiO_2 and P-25). This can be ascribed to the synergetic effect between the anatase and rutile nanoparticles, which enhances the electron-hole separation and thus increases the photocatalytic activity[25,26]. Similar behavior has been reported for bi-phase TiO_2 photocatalysts under an optimum rutile/anatase ratio in different contaminants including naphthalene, hexane and methanol. Ohno et al.[25] reported that bi-phase powder shows higher activity than pure anatase or pure rutile powder in naphthalene, which they attributed to the synergetic effect between anatase and rutile powders, assuming that rutile particles are responsible for the oxidation of naphthalene, while the anatase particles are responsible for the reduction of oxygen.

Wu et al.[26] reported that the photocatalytic oxidation of hexane and methanol in TiO_2 nanoparticles is dependent on the phase composition of the photocatalyst, where an optimum anatase/rutile ratio (85-88/15-12) is essential to attain higher photocatalytic efficiency for the bi-phase photocatalyst. However, Yang et al.[27] reported that the photocatalytic activity of bi-phase powder containing 65% rutile phase in methyl orange is inferior to pure anatase phase TiO_2 powder.

These results illuminate that the use of surfactants does not always enhance the photocatalytic activity although it may improve the size of the synthesized nanoparticles. In addition, the photocatalytic activity depends on many complicated factors including the particle size, specific surface area, particle size distribution, porosity and phase composition, which should be interconnected to each other. However, the crystal structure, the change in the band gap, and the electronic state are the most important variables in determining the photocatalytic activity.

CONCLUSION

Titanium dioxide (TiO_2) nanoparticles were synthesized by sol-gel technique with and without the addition of surfactant. Cetyltrimethylammonium bromide (CTAB) and polyvinylpyrolidone (PVP) were used as particle size inhibitors. Characterization results showed that the prepared nanoparticles show different particle sizes, particle size distribution and phase composition. Samples prepared by using CTAB as surfactant reveal pure anatase phase structure with uniform size distribution of about 13 nm, while samples prepared without the introduction of surfactant and those prepared by using PVP show a bi-phase structure with different rutile concentration and particle size distribution. The photocatalytic activity of the prepared powders in methyl orange was measured and compared to that of Degussa TiO_2 nanopowder. The highest degradation efficiency was obtained by the photocatalyst prepared with PVP as surfactant; while the lowest degradation efficiency was obtained by the photocatalyst prepared using CTAB. The bi-phase powders show higher degradation efficiency compared to pure anatase phase powders, due to a synergetic effect between anatase and rutile powders, which enhances the electron-hole separation and thus increases the photocatalytic activity.

ACKNOWLEDGMENTS

The authors gratefully acknowledge the financial support for this work from the Fok Ying Tong Education Foundation (Grant No. 91050) and the National Natural Science Foundation of China (Grant No. 50202007).

REFERENCES

[1] K.Pan, Q.Zhang, Q.Wang, Z.Liu, D.Wang, J.Li, Y. Bai; Thin Solid Films, **515**, 4085 **(2007)**

[2] S.Pavasupree, S.Ngamsinlapasathian, M.Nakajima, Y.Suzuki, S.Yoshikawa; J.Photochem.Photobiol.: A, **184**, 163 **(2006)**.

[3] K.M.Leea, V.Suryanarayanan, K.C.Hoa; Sol.Energ.Mater.Sol.Cells, **90**, 2398 **(2006)**.

[4] S.Ngamsinlapasathian, T.Sreethawong, Y.Suzuki, S.Yoshikawa; Sol.Energ.Mater.Sol.Cells, **86**, 269 **(2005)**.

Full Paper

[5] J.H.Yoon, S.R.Jang, R.Vittal, J.Lee, K.J.Kim; J. Photochem.Photobiol.A, **180**, 184 **(2006)**.

[6] P.D.Cozzoli, A.Kornowski, H.Weller; J.Am.Chem. Soc., **125**, 14539 **(2003)**.

[7] K.Zakrzewska; Thin Solid Films, **391**, 229 **(2001)**.

[8] A.Hagfeldt, M.Gratzel; Chem.Rev., **95**, 49 **(1995)**.

[9] S.Sakthivel, H.Kisch; Angew.Chem.Int.Ed., **42**, 4908 **(2003)**.

[10] H.Kominami, S.Y.Murakami, M.Kohno, Y.Kera, K. Okada, B.Ohtani; Phys.Chem.Chem.Phys., **3**, 4102 **(2001)**.

[11] M.R.Hoffmann, S.T.Martin, W.C.Choi, D.W. Bahnemann; Chem.Rev., **95**, 69 **(1995)**.

[12] A.L.Linsebigler, G.Lu Jr., J.T.Yates; Chem.Rev., **95**, 735 **(1995)**.

[13] M.A.Fox, M.T.Dulay; Chem.Rev., **93**, 341 **(1993)**.

[14] A.Fujishima, K.Honda; Nature, **238**, 37 **(1972).**

[15] Y.Xie, C.Yuan, X.Z.Li; Colloids and Surfaces A, **252**, 87 **(2005)**.

[16] B.Jiang, H.Yin, T.Jiang, Y.Jiang, H.Feng, K.Chen, W.Zhou, Y.Wada; Mater.Chem.Phy., **98**, 231 **(2006)**.

[17] P.K.Khanna, N.Singh, S.Charan; Mater.Lett., **61**, 4725 **(2007)**.

[18] S.Qourzal, A.Assabbane, Y.Ait-Ichou; J. Photochem.Photobiol.A, **163**, 317**(2004)**.

[19] J.Xu, L.Li, Y.Yan, H.Wang, X.Wang, X.Fu, G.Li; J. Coll.Interf.Sci., **318**, 29 **(2008)**.

[20] Y.M.Jun, M.F.Casula, S.Y.Kim; J.Am.Chem.Soc., **125**, 15981 **(2003)**.

[21] M.P.Pileni; Nature Materials, **2**, 145 **(2003)**.

[22] Y.V.Kolen'ko, B.R.Churagulov, M.Kunst, L. Mazerolles, C.Colbeau-Justin; Appl.Catal.: B, **54**, 51 **(2004)**.

[23] R.Leung, M.J.Hou, D.O.Shah, D.T.Wasan, M.E. Ginn, D.O.Shah; Surfactant Science Series, Marcel Dekker, New York, **28**, **(1988)**.

[24] S.Pavasupree, J.Jitputti, S.Ngamsinlapasathian, S. Yoshikawa; Mater.Res.Bul., **43**, 149 **(2008)**.

[25] T.Ohno, K.Tokieda, S.Higashida; Appl.Catal.A, **244**, 383 **(2003)**.

[26] C.Wu, Y.Yue, X.Deng; Catal.Today, **93-95**, 863 **(2004)**.

[27] H.Yang, K.Zhang, R.Shi, X.Li, X.Dong, Y.Yu; J. Alloy Comp., **413**, 302 **(2006)**.